Gina Brown, FRCR
Catherine J. Richards, FRCPath
Michael W. Bourne, FRCR
Robert G. Newcombe
Andrew G. Radcliffe, FRCS
Nicholas S. Dallimore, FRCPath
Geraint T. Williams, FRCPath

# Morphologic Predictors of Lymph Node Status in Rectal Cancer with Use of High-Spatial-Resolution MR Imaging with Histopathologic Comparison[1]

**Index terms:**
Lymphatic system, MR, 99.129411
Lymphatic system, neoplasms, 99.33
Rectum, neoplasms, 757.321

**Published online**
10.1148/radiol.2272011747
**Radiology 2003;** 227:371–377

**Abbreviation:**
SE = spin echo

[1] From the University Hospital of Wales and Llandough Hospital NHS Trust, University of Wales College of Medicine, Cardiff. From the 1999 RSNA scientific assembly. Received October 26, 2001; revision requested January 15, 2002; final revision received July 1; accepted August 9. Supported by the NHS Wales Office for Research and Development in Health and Social Care. G.B. supported by a Royal College of Radiologists BUPA research fellowship. **Address correspondence to** G.B., Department of Radiology, Royal Marsden NHS Trust, Downs Rd, Sutton, Surrey SM2 5PT, England (e-mail: *gina.brown@rmh.nthames.nhs.uk*).

**Author contributions:**
Guarantors of integrity of entire study, G.T.W., M.W.B.; study concepts, G.B.; study design, G.B., G.T.W.; literature research, G.B.; clinical studies, A.G.R., N.S.D., G.B., G.T.W., M.W.B.; data acquisition, G.B., M.W., C.J.R., N.S.D.; data analysis/interpretation, G.B., R.G.N.; statistical analysis, G.B., R.G.N.; manuscript preparation, G.B., R.G.N., G.T.W.; manuscript definition of intellectual content, G.B., G.T.W.; manuscript editing, G.B., G.T.W., R.G.N.; manuscript revision/review, G.B., M.W.B., G.T.W., R.G.N.; manuscript final version approval, all authors.



**PURPOSE:** To evaluate signal intensity and border characteristics of lymph nodes at high-spatial-resolution magnetic resonance (MR) imaging in patients with rectal cancer and to compare these findings with size in prediction of nodal status.

**MATERIALS AND METHODS:** Forty-two patients who underwent total mesorectal excision of the rectum to determine if they had rectal carcinoma were studied with preoperative thin-section MR imaging. Lymph nodes were harvested from 42 transversely sectioned surgical specimens. The slice of each lymph node was carefully matched with its location on the corresponding MR images. Nodal size, border contour, and signal intensity on MR images were characterized and related to histologic involvement with metastases. Differences in sensitivity and specificity with border or signal intensity were calculated with CIs by using method 10 of Newcombe.

**RESULTS:** Of the 437 nodes harvested, 102 were too small (<3 mm) to be depicted on MR images, and only two of these contained metastases. In 15 (68%) of 22 patients with nodal metastases, the size of normal or reactive nodes was equal to or greater than that of positive nodes in the same specimen. Fifty-one nodes were above the area imaged, and seven of these contained metastases. The diameter of benign and malignant nodes was similar; therefore, size was a poor predictor of nodal status. If a node was defined as suspicious because of an irregular border or mixed signal intensity, a superior accuracy was obtained and resulted in a sensitivity of 51 (85%) of 60 (95% CI: 74%, 92%) and a specificity of 216 (97%) of 221 (95% CI: 95%, 99%).

**CONCLUSION:** Prediction of nodal involvement in rectal cancer with MR imaging is improved by using the border contour and signal intensity characteristics of lymph nodes instead of size criteria.


Preoperative assessment of lymph node status in patients with rectal cancer is important for a number of reasons. First, the number of involved nodes has an influence on the prognosis of the patient (1,2). Second, the presence of tumor-containing lymph nodes near the mesorectal fascia (which forms the conventional surgical circumferential resection margin) increases the risk of recurrence (3), unless the standard excision plane is altered. Nodes lying outside the mesorectal fascia may require extended lymphadenectomy to achieve clearance of the tumor (4,5). Those that remain unresected may be responsible for local recurrence, despite apparently clear surgical resection margins (6). The use of neoadjuvant preoperative therapy may be influenced by the presence of tumor-containing nodes close to the potential resection plane. Finally, the ability to determine reliably

node-negative status before surgery could result in less aggressive surgery and preoperative therapy in some patients.

Existing imaging criteria for nodal positivity vary. Some authors regard any visible node in the perirectal fat as positive (7), while others employ size criteria with cutoff values for nodal positivity that range from 3 to 10 mm (8,9). Indeed, while the majority of published studies use size criteria to predict nodal status, there is no agreement on what discriminant value is to be used; however, it is accepted that the use of size criteria alone will result in false-positive diagnoses (10). Although the internal architecture of nodes has been studied with endoluminal ultrasonography (US) (11,12), to our knowledge the specific morphologic appearances of lymph nodes in rectal cancer on magnetic resonance (MR) images have not been evaluated. This study was undertaken to evaluate the signal intensity and border characteristics of nodal morphology in patients with rectal cancer by using high-spatial-resolution MR images and to compare the signal intensity and border characteristics with nodal size as predictors of final nodal status.

## MATERIALS AND METHODS

This study was performed according to a protocol approved by the Ethics Committee of our institution, and informed consent was obtained from each patient. Forty-two consecutive patients who underwent total mesorectal excision of the rectum with a biopsy to determine if they had rectal carcinoma were studied. MR imaging was performed with a 1.5-T unit (Horizon Advantage, version 5.62; GE Medical Systems, Milwaukee, Wis) with a four-element pelvic phased-array wraparound surface coil. All patients were imaged in the supine position. Neither intravenous antiperistaltic agents nor contrast agents were administered. A coronal localizing image was obtained to select transverse and sagittal images with a T2-weighted fast spin-echo (SE) sequence (repetition time msec/echo time msec, 2,500–5,000/100; 256 × 256 matrix, echo train length, 16; four signals acquired; sequence duration, 3–5 minutes). These images were obtained with a 24-cm field of view and 5-mm-thick sections with no intersection gap. The sagittal images were used to plan oblique high-spatial-resolution (in-plane resolution, 0.6 × 0.6 mm) transverse imaging. The images were acquired in a plane orthogonal to the tumor and rectal wall by using a T2-weighted fast SE sequence (2,500–5,000/100; 256 × 256 matrix; echo train length, 16). All images were obtained with a 16-cm field of view and 3-mm-thick sections with no intersection gap and four signals acquired. The sequence duration lasted from 8 to 15 minutes (mean, 11 minutes). T1-weighted imaging was not performed, as it contributed no additional information to the analysis.

After they underwent MR imaging, all patients underwent surgical resection of their tumors with a total mesorectal excision.

### Image Interpretation

The MR images of the nodes were characterized according to the following parameters.

*Nodal size criteria.*—The maximum diameter of the lymph node was measured in millimeters. Images were zoomed at the MR imaging workstation (Advantage, version 3.1; GE Medical Systems), and measurements were made with workstation electronic callipers.

*Border contour and signal intensity.*—The borders of each node were classified as either "smooth and well defined" or "irregular and ill defined". The signal intensity within a given node was compared with that of the primary tumor. A note was made if the imaged node appeared to be hypointense, isointense, or hyperintense relative to the tumor. The observers also recorded whether the signal intensity within the node was uniform and homogeneous or mixed with foci of different signal intensities.

After the appearance of the node was characterized, interobserver agreement between the two independent observers (M.W.B. and G.B., with 5 and 10 years, respectively, of experience in MR imaging) was measured.

### Nodal Comparison

After surgical resection of the tumors, the specimens were again imaged with the same preoperative protocol after they were fixed in formalin. A radiologist (G.B.) was present during the dissection of the rectal specimens. Each specimen was sliced transversely at 3-mm intervals, and the slices were matched with in vivo MR images and specimen MR images to obtain a precise slice-for-section match. The slices were photographed, and all visible lymph nodes were harvested. The slice and location of each lymph node were matched with its corresponding MR image (when visible) to enable a node-for-node comparison of MR images and histologic findings. Slices from all lymph nodes were stained with hematoxylin-eosin.

### Histologic Assessment

The following histologic observations were recorded by one of three histopathologists (C.J.R., N.S.D., G.T.W.) for each node. First, the status of each node was classified as being normal, reactive, or involved with a metastatic rectal adenocarcinoma. Second, if a tumor nodule 3 mm or more in diameter was identified in the perirectal or pericolic fat, and there was no histologic evidence of residual nodal tissue, it was classified as a regional lymph node metastasis, in accordance with the rules of TNM staging (13). Finally, the maximum diameter of the node was measured in millimeters.

### Statistical Methods

Sensitivity and specificity of nodal size, border contour, and signal intensity at MR imaging as predictors of nodal involvement were determined with reference to the corresponding histologically determined nodal status as the standard. These were determined with 95% CIs calculated by using the method of Wilson (14). Differences in sensitivity and specificity with the nodal border or signal intensity versus nodal size were calculated with CIs by using method 10 of Newcombe (15) and compared graphically (16). Interreader agreement for the MR imaging assessment of border characteristics and signal intensity was assessed by using the $\kappa$ statistic (17).

## RESULTS

Table 1 summarizes the MR imaging characteristics versus the histologic findings in 437 lymph nodes harvested from the rectal cancer resection specimens of 42 patients. Of these 437 lymph nodes, 102—all less than 3 mm in diameter—were not identified on MR images (two contained metastases). An additional 51 lymph nodes were above the area imaged with high-spatial-resolution MR imaging (seven contained metastases). Two hundred eighty-four lymph nodes were therefore available for evaluation of MR imaging appearances in the prediction of nodal involvement.

### Nodal Size Criteria

The size at MR imaging of lymph nodes that contained metastases varied greatly,

**TABLE 1**
**MR Imaging Characteristics versus Histologic Findings in 437 Lymph Nodes**

| MR Imaging Characteristics | Total | Histologic Findings | | |
|---|---|---|---|---|
| | | Negative | Reactive | Positive |
| Above the area imaged | 51 | 37 | 7 | 7 |
| Not seen | 102 | 96 | 4 | 2 |
| Size | | | | |
| ≤5 mm | 229 | 159 | 35 | 35 |
| >5 mm | 55 | 15 | 15 | 25 |
| Signal intensity relative to tumor | | | | |
| Hyperintense | 75 | 46 | 26 | 3 |
| Isointense | 91 | 69 | 5 | 17 |
| Hypointense | 83 | 54 | 18 | 11 |
| Mixed | 32 | 3 | 0 | 29 |
| Border contour | | | | |
| Smooth | 232 | 168 | 49 | 15 |
| Irregular | 49 | 4 | 0 | 45 |

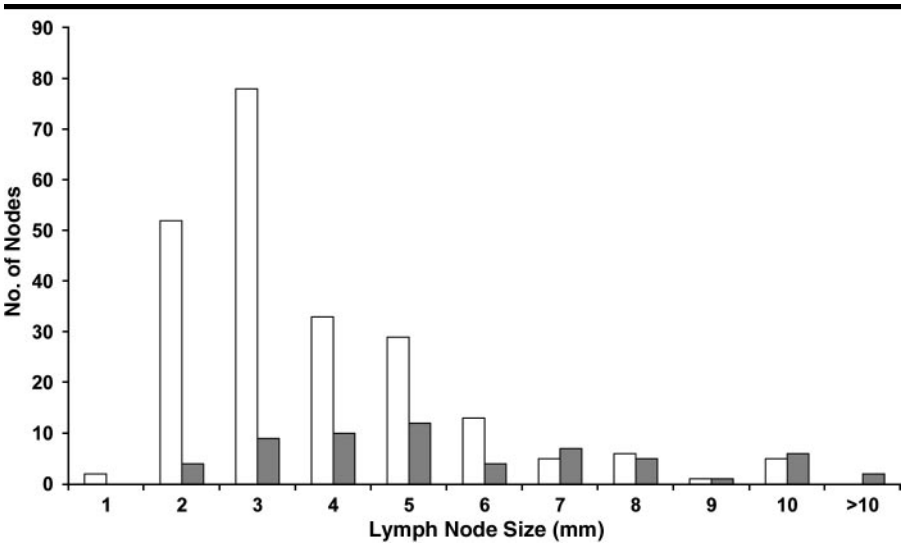


**Figure 1.** Histogram shows the number of normal (white bars) and malignant (gray bars) nodes seen on MR images, according to diameter (which is measured in millimeters).

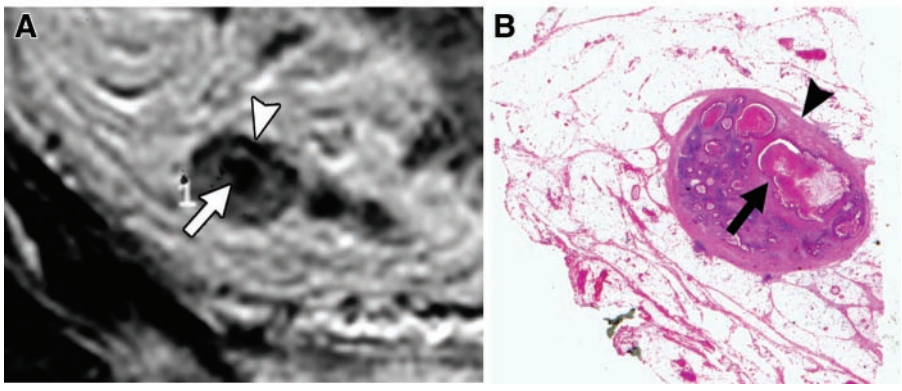


**Figure 2.** *A,* T2-weighted fast SE transverse MR image (2,500/100) shows a node of mixed signal intensity with a low-signal-intensity rim (arrowhead). A focus of low signal intensity (arrow) is demonstrated within the predominantly intermediate-signal-intensity node. *B,* Histologic slice of the corresponding node shows low-signal-intensity rim seen on MR image that corresponds to the normal lymph node capsule (arrowhead). Within the node, there is tumor (arrow) with widespread necrosis in the area corresponding to the low-signal-intensity area seen on the MR image. (Hematoxylin-eosin stain; original magnification, ×6.)

and 35 (58%) of 60 positive lymph nodes were less than 5 mm in diameter (Fig 1). MR measurement of nodal diameters ranged from 2 to 10 mm in 119 benign nodes from 20 patients with node-negative status and from 3 to 15 mm in 60 cancerous nodes from 22 patients with node-positive status. Furthermore, in 15 (71%) of 21 patients with lymph node metastases, the size of normal or reactive nodes was similar to or greater than the smallest positive node in the same specimen. A cutoff of 5 mm gave optimal sensitivity and specificity for nodal status (81% and 68%, respectively) in the 42 patients. The corresponding sensitivity and specificity for nodal detection was 25 (42%) of 60 and 194 (87%) of 224, respectively. A cutoff of greater than 10 mm would give a sensitivity of two (3%) of 60 for nodal detection and a specificity of 224 (100%) of 224, while a cutoff of greater than 3 mm would give a sensitivity for nodal detection of 47 (78%) of 60 and a specificity of 132 (59%) of 224. Whatever cutoff is used, the overall predictive value of MR size is poor because of substantial overlap in size between nodes that are benign and malignant.

## Signal Intensity and Border Characteristics

In three of 284 nodes depicted by MR imaging (all >3 mm), the signal intensity and border characteristics could not be evaluated further due to image degradation caused by motion artifact. The remaining 281 nodes were assessed for signal intensity (relative to the primary tumor) and border characteristics. Of 75 hyperintense nodes on MR images, only three (4%) were malignant. Of 91 isointense nodes, seven (8%) were malignant. Of 83 hypointense nodes, 11 (13%) were malignant. However, of 32 nodes containing mixed signal intensity—namely, foci of different signal intensities present within the node (Fig 2)—29 (91%) were malignant. Use of mixed signal intensity alone as a marker for nodal involvement gave a low sensitivity of 29 (48%) of 60 but a high specificity of 218 (99%) of 221. Areas of mixed signal intensity on MR images corresponded to tumor deposits with areas of necrosis or extracellular mucin (Fig 3) at histologic examination.

Evaluation of the border contour of lymph nodes yielded better predictive power. Fifteen (6%) of 232 nodes with smooth borders contained metastases compared with 45 (92%) of 49 nodes with irregular borders (Fig 4), which yielded a sensitivity of 45 (75%) of 60 and a specificity of 217 (98%) of 221.

Thus, virtually all normal or reactive lymph nodes were characterized by uniform signal intensity and smooth, sharply demarcated borders (Fig 5). Twenty-eight (57%) of 49 nodes with an irregular border were completely replaced by tumor with no visible lymphoid tissue present (all were >3 mm in diameter).

When lymph node border characteristics and signal intensity were combined so that a node was regarded as positive if either an irregular border or a mixed signal intensity was demonstrated, the sensitivity improved, and there was a high specificity. Metastases were demonstrated in 51 (91%) of 56 nodes (95% CI: 81%, 96%) with either an irregular border or a mixed signal intensity. Conversely, only nine (4%) of 225 nodes (95% CI: 2.1%, 7.4%) with smooth borders and uniform signal intensity contained metastases. This corresponded with a sensitivity for metastatic nodal detection of 51 (85%) of 60 (95% CI: 74%, 92%) and a specificity of 216 (98%) of 221 (95% CI: 95%, 99%).

If we used this model, there would have been nine false-negative nodes and five false-positive nodes. The nine false-negative nodes occurred in five patients. One patient had five false-negative nodes that were all 3 mm or less in diameter and of homogeneous low signal intensity with smooth borders. In three patients, there were other involved nodes that had been correctly identified according to their MR appearance. In two patients, the only histologically involved node was not demonstrated at MR imaging. Only one of these nodes was greater than 5 mm, indicating that adding size information would not greatly help to reduce false-negative results or improve specificity. The five false-positive nodes came from four patients. One patient had two false-positive nodes, both measuring 3 mm in diameter with mixed signal intensity. Both of these nodes were histologically normal, and the reason for the mixed signal intensity is unclear. Two patients had a single 3-mm false-positive node with an irregular border. One patient had a 5-mm node with an irregular border. Three of these four patients had other histologically malignant nodes. Applying the model based on lymph node contour and MR signal intensity for identifying patients (as opposed to individual nodes) with nodal metastases gave a sensitivity of 17 (77%) of 22 (95% CI: 57%, 90%) and a specificity of 19 (95%) of 20, (95% CI: 76%, 99%). Interobserver agreement for assigning nodes into involved or noninvolved groups with this

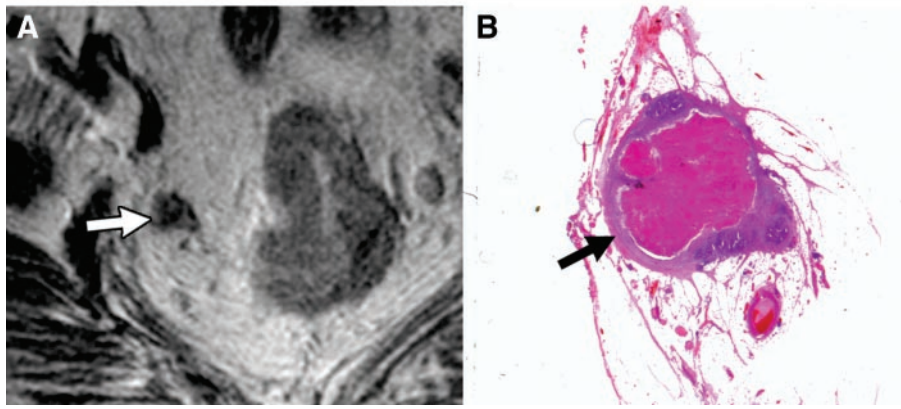


**Figure 3.** *A,* T2-weighted fast SE transverse MR image (2,500/100) through the upper portion of the rectum. A node with an irregular border (arrow) located close to the right lateral mesorectal margin contains mixed signal intensity. *B,* Photomicrograph shows corresponding node (arrow) harvested from the right lateral mesorectal margin of the specimen contains proteinaceous extracellular mucin. (Hematoxylin-eosin stain; original magnification, ×6.)

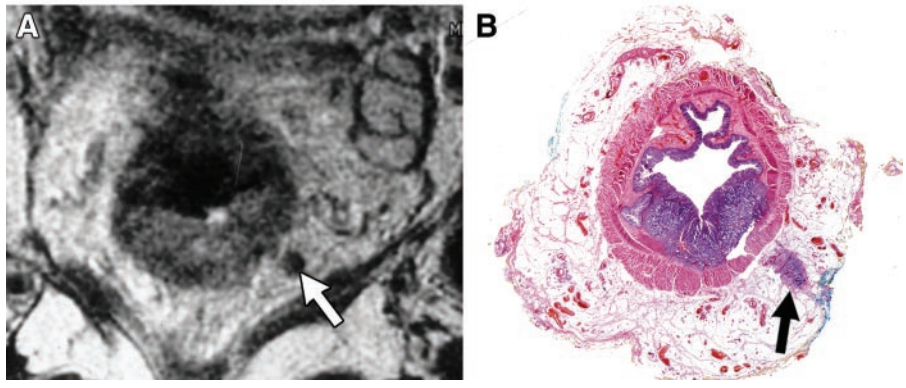


**Figure 4.** *A,* T2-weighted fast SE transverse MR image (2,500/100) of the lower portion of the rectum. A low-signal-intensity node (arrow) with irregular borders is demonstrated on the left posterolateral border of the mesorectum. *B,* Corresponding histologic wholemount slice from the total mesorectal excision specimen shows tumor deposit (arrow) with an irregular border within the mesorectum. Since there is no visible nodal tissue, it is indistinguishable from an extranodal deposit. This is classified as node positive with the TNM classification (11). (Hematoxylin-eosin stain; original magnification, ×1.)

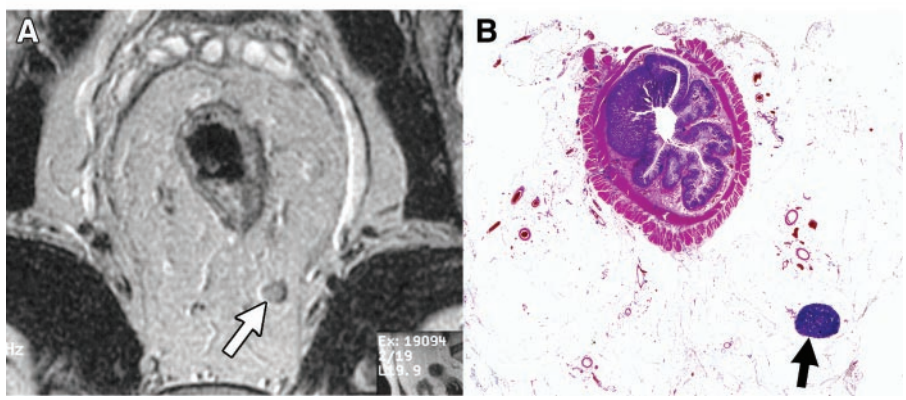


**Figure 5.** *A,* T2-weighted fast SE transverse MR image (>2,500/100) through the middle portion of the rectum. A high-signal-intensity node with smooth borders (arrow) of homogeneous signal intensity is demonstrated close to the right posterolateral border of the mesorectum. *B,* Corresponding histologic wholemount slice from total mesorectal excision revealed benign node (arrow). (Hematoxylin-eosin stain; original magnification, ×1.)

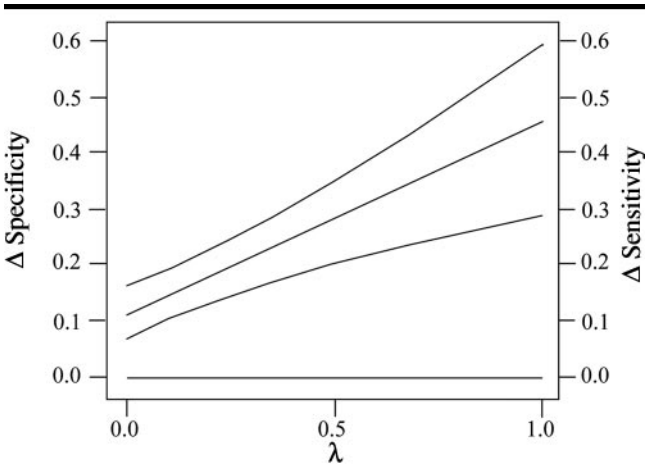


**Figure 6.** Based on reference 16, graph compares sensitivity and specificity for metastatic nodal detection simultaneously between an assessment of morphology (presence of an irregular border or mixed signal intensity) and node size (defined by a cutoff of >5 mm). Differences in sensitivity and specificity are plotted at the vertical axes at $\lambda = 1$ and $\lambda = 0$, respectively, with confidence limits shown above and below. λ incorporates the effects of the prevalence of the abnormality and the "costs" of misclassification expressed by relative importance of false-positive and false-negative results. The diagonal line plots how λ weighting alters the difference in sensitivity and specificity between the two tests. In most applications, the point where the line crosses the horizontal axis would indicate the circumstances under which one test would be regarded as the better one. This chart shows that the whole of the line and its confidence region lie above the horizontal axis, indicating a strong preference for morphologic criteria rather than size, irrespective of prevalence and relative costs.

**TABLE 2**
**Existing Criteria for Identification of Nodal Tumor Involvement**

| Source | Criteria for Positive Nodes |
|---|---|
| Kusunoki et al (18), 1994 | Diameter >8 mm |
| Schnall et al (10), 1994 | Any non–fat-containing node |
| Okizuka et al (7), 1996 | Any recognizable node in perirectal fat, regardless of diameter |
| Indinnimeo et al (19), 1996 | Diameter ≥5 mm |
| Zerhouni et al (9), 1996 | Long axis diameter >10 mm or greater than usual number of nodes |
| Vogl et al (8), 1997 | Size >3 mm |

model was 85%, with a κ value of 0.71 (95% CI: 55%, 79%).

Figure 6 (based on a method of statistical analysis described in reference 16) simultaneously compares the nodal sensitivity and specificity between our proposed assessment of morphology (in which a node is defined as suspicious if either irregular or returning a mixed signal intensity) and node size (defined by a cutoff of >5 mm). There are significant differences for both sensitivity (43%; 95% CI: 28%, 56%) and specificity (11%; 95% CI: 6%, 16%), both favoring morphology. The figure shows how this results in an unequivocal advantage with use of our criterion rather than size in predicting nodal involvement. The differences in sensitivity and specificity are plotted at the vertical axes ($\lambda = 1$ and $\lambda = 0$, respectively), with confidence limits shown above and below these points. The mixing parameter λ is designed to incorporate both the prevalence of abnormality in the series to which the tests are to be applied and the relative costs or regrets resulting from the two possible types of misclassification. If false-negative results are regarded as a much more serious problem than false-positive results, and the prevalence of nodal positivity is high, λ will approach 1. Conversely, if concern centers on overstaging while the prevalence of nodal positivity is low, λ will approach 0. The diagonal line indicates how a suitably weighted average of the differences in sensitivity and specificity between the two tests depends on the value of λ. The upper and lower curves give confidence limits for this quantity for each value of λ. In most applications, we would then identify where the line and the curves cut the horizontal axis. This would help indicate under what circumstances each test should be used. In this instance, the whole of the line and its confidence region lie above the horizontal axis, which indicates a strong preference for the morphologic criterion, irrespective of prevalence and relative costs.

## DISCUSSION

Nearly all published MR imaging studies of rectal cancer have used size as a criterion for predicting nodal involvement (7–10,18,19) (Table 2), although there is little consistency in the size used to discriminate between benign and malignant lymph nodes. A similar situation pertains for endoscopic US (20). Moreover, there is little hard evidence to support the use of any single size criterion, and, to our knowledge no studies that meticulously match individual lymph nodes seen on images with their precise histologic counterparts have been reported. Any proposed cutoff value has been the result of finding a compromise between sensitivity and specificity (7–10,19). A cutoff value of 10 mm gives high specificity but low sensitivity (9), whereas the reverse is true if a cutoff of 3 mm is employed (8). Our study has led us to conclude that no particular size cutoff is useful in predicting nodal status. This conclusion is supported by a histologic survey of over 12,000 lymph nodes in patients with rectal cancer that showed considerable size overlap between normal or reactive nodes and those that contained metastases (21). Schnall et al (10) used endorectal MR imaging and noted that positive lymph nodes varied substantially in size; five of 12 nodes that measured 5 mm or less contained a tumor. Dworak (22), in a histologic survey, found that the only positive lymph nodes in 31 of 98 patients with rectal cancer measured less than 5 mm.

Given that small (<5 mm) mesorectal lymph nodes in patients with rectal cancer may contain metastases (15% in our study), it is pertinent to consider how reliably they can be identified with the

high-spatial-resolution MR imaging technique that we employed. The ability to identify nodes less than 5 mm in diameter is recognized as a substantial limitation of determining the stage of cancer with endoluminal US (20), since only 13% of positive lymph nodes that measured less than 5 mm in diameter were detected in one series (23). We found that 23% of the nodes harvested from resection specimens were not identified with MR imaging, but these were all less than 3 mm and only two of the 102 contained metastases. On the other hand, our technique enabled us to identify many nodes that measured 2–5 mm and correctly predict the presence of metastases in some nodes based on irregular contour. While its power to resolve such small nodes is clearly suboptimal, it would seem that MR evaluation of nodes by using the criteria we have developed will result in understaging in very few patients. Nevertheless, although we did not formally evaluate patients who underwent local resection of rectal cancer in our study, the inability to detect microscopic metastases in all lymph nodes suggests that an MR examination that is negative for metastases should not be used to select patients for local resection surgery.

An important observation made in endoluminal US studies (24,25) is that the internal texture of an imaged node may correlate better with the presence of metastases than nodal size, and that inhomogeneity and hilar reflectivity are important discriminators of nodal status. Katsura et al (26) noted that the specificity of endoluminal US could be improved if the echogenicity of a node was considered in addition to its size. Metastases were more common in nodes of mixed intranodal echogenicity than in those of uniform hyperechogenicity. Our study has shown the value of applying these observations to high-spatial-resolution MR imaging of lymph node status, and the demonstration of intranodal heterogeneity of signal intensity (ie, mixed signal intensity) is again shown to be a highly specific discriminant. Lee et al (27) used MR imaging in vitro at 9.4 T to demonstrate that the detailed microstructure and internal morphology of normal nodes are best demonstrated on T2-weighted images. It is a common misconception that all lymph nodes of high signal intensity contain fat. While fat replacement of nodes is well recognized in the axilla and inguinal nodes, the presence of intranodal fat is not a feature of perirectal lymph nodes. The high signal intensity is presumed to represent fluid within lymphoid follicles. They are surrounded by a low-signal-intensity capsule and contain relatively low-signal-intensity fibrous trabeculae–containing medullary sinuses (20). By using careful node-for-node correlation with histopathologic findings, we now show that high-spatial-resolution MR images allow the internal morphology of pathologic nodes to be evaluated. Furthermore, we found that nodes with mixed signal intensity are likely to contain areas of necrosis or extracellular mucin that correspond to metastatic adenocarcinoma. We are not the first to use intranodal signal intensity in the evaluation of nodal disease in rectal cancer. Schnall et al (10) suggested that a low nodal signal intensity might be a predictor of tumor involvement; however, we found that this feature alone did not correlate with nodal status unless mixed-signal-intensity foci were demonstrated within the node. Evaluation of intranodal signal intensity homogeneity requires high-quality images that are free of movement artifacts, and because these qualities are difficult to obtain in small nodes, we do not feel able to make this assessment in nodes less than 3 mm.

A potential limitation of this study is that an evaluation of the endorectal coil was not included; however, we believe that endorectal coil imaging has a limited role in the routine local determination of the stage of rectal cancer because tumors that are bulky or cause strictures of the rectum prevent endorectal coil insertion. Tumors of the upper rectum are beyond the reach of the endorectal coil, and its inherent small field of view limits the assessment to a small area of perirectal fat.

An interesting result of our study was the very high specificity of 98% (217 of 221) and moderate sensitivity of 75% (45 of 60) of the lymph node border characteristics on MR images. Curiously, this feature does not appear to have been evaluated previously, despite the fact that it is well recognized that partial or complete nodal replacement with a tumor results in gross distortion, and extranodal extension in incompletely involved nodes leads to irregularity of the surrounding capsule. The high spatial resolution of the MR imaging technique in assessing this feature, combined with the heterogeneity of the intranodal signal intensity, produces a powerful predictor of lymph node status that shows good reproducibility between observers and is independent of, and greatly superior to, lymph node size. As evidence accrues for the advantages of preoperative therapy (28,29) over postoperative adjuvant therapy in patients with locally advanced rectal cancer, the importance of accurately determining the stage of cancer in the mesorectum with imaging techniques prior to surgery will increase. Indeed, if such preoperative local-regional and systemic treatments result in substantial tumor downstaging, examination of resection specimens will become displaced as the standard for defining the original tumor stage, and preoperative MR imaging will assume greater importance. Inability to predict nodal status in patients with rectal cancer is viewed as an important limitation of current imaging techniques.

Our study findings show that by using high-spatial-resolution MR imaging, morphologic criteria employing the signal intensity and border characteristics of nodes are superior to size in predicting nodal status; this technique holds considerable promise for improving preoperative staging in patients with rectal cancer.

**Acknowledgments:** We thank our collaborators, Timothy S. Maughan, MD, FRCR, Jane S. Blethyn, FRCR, Ceri J. Phillips, and Shan Davies for their contributions to this project. We are indebted to histopathology staff at Llandough Hospital and the University Hospital of Wales (Patricia Thomas and Simon Iles) and to the MR radiographers at the University Hospital of Wales (Diane Fletcher, DCR, and Joanne Sayman, DCR).

**References**

1. Wolmark N, Fisher B, Wieand HS. The prognostic value of the modifications of the Dukes' C class of colorectal cancer: an analysis of the NSABP clinical trials. Ann Surg 1986; 203:115–122.
2. Tang R, Wang JY, Chen JS, et al. Survival impact of lymph node metastasis in TNM stage III carcinoma of the colon and rectum. J Am Coll Surg 1995; 180:705–712.
3. Adam IJ, Mohamdee MO, Martin IG, et al. Role of circumferential margin involvement in the local recurrence of rectal cancer. Lancet 1994; 344:707–711.
4. Billingham RP. Extended lymphadenectomy for rectal cancer: cure vs quality of life. Int Surg 1994; 79:11–22.
5. Suzuki K, Muto T, Sawada T. Prevention of local recurrence by extended lymphadenectomy for rectal cancer. Surg Today 1995; 25:795–801.
6. Moreira LF, Hizuta A, Iwagaki H, Tanaka N, Orita K. Lateral lymph node dissection for rectal carcinoma below the peritoneal reflection. Br J Surg 1994; 81:293–296.
7. Okizuka H, Sugimura K, Yoshizako T, Kaji Y, Wada A. Rectal carcinoma: prospective comparison of conventional and gadopentetate dimeglumine enhanced fat-suppressed MR imaging. J Magn Reson Imaging 1996; 6:465–471.
8. Vogl TJ, Pegios W, Mack MG, et al. Accuracy of staging rectal tumors with contrast-enhanced transrectal MR imaging.

AJR Am J Roentgenol 1997; 168:1427–1434.
9. Zerhouni EA, Rutter C, Hamilton SR, et al. CT and MR imaging in the staging of colorectal carcinoma: report of the Radiology Diagnostic Oncology Group II. Radiology 1996; 200:443–451.
10. Schnall MD, Furth EE, Rosato EF, Kressel HY. Rectal tumor stage: correlation of endorectal MR imaging and pathologic findings. Radiology 1994; 190:709–714.
11. Hildebrandt U, Klein T, Feifel G, et al. Endosonography of pararectal lymph nodes: in vitro and in vivo evaluation. Dis Colon Rectum 1990; 33:863–868.
12. Hildebrandt U, Feifel G. Importance of endoscopic ultrasonography staging for treatment of rectal cancer. Gastrointest Endosc Clin N Am 1995; 5:843–849.
13. Sobin L, Wittekind C. TNM classification of malignant tumors. New York, NY: Wiley, 1997; 227.
14. Wilson EB. Probable inference, the law of succession, and statistical inference. J Am Stat Assoc 1927; 22:209–212.
15. Newcombe RG. Interval estimation for the difference between independent proportions: comparison of eleven methods. Stat Med 1998; 17:873–890.
16. Newcombe RG. Simultaneous comparison of sensitivity and specificity of two tests in the paired design: a straightforward graphical approach. Stat Med 2001; 20:907–915.
17. Altman DG. Inter-rater agreement. In: Practical statistics for medical research. London, England: Chapman & Hall, 1990; 403–407.
18. Kusunoki M, Yanagi H, Kamikonya N, et al. Preoperative detection of local extension of carcinoma of the rectum using magnetic resonance imaging. J Am Coll Surg 1994; 179:653–656.
19. Indinnimeo M, Grasso RF, Cicchini C, et al. Endorectal magnetic resonance imaging in the preoperative staging of rectal tumors. Int Surg 1996; 81:419–422.
20. Detry RJ, Kartheuser AH, Lagneaux G, Rahier J. Preoperative lymph node staging in rectal cancer: a difficult challenge. Int J Colorectal Dis 1996; 11:217–221.
21. Dworak O. Morphology of lymph nodes in the resected rectum of patients with rectal carcinoma. Pathol Res Pract 1991; 187:1020–1024.
22. Dworak O. Number and size of lymph nodes and node metastases in rectal carcinomas. Surg Endosc 1989; 3:96–99.
23. Spinelli P, Schiavo M, Meroni E, et al. Results of EUS in detecting perirectal lymph node metastases of rectal cancer: the pathologist makes the difference. Gastrointest Endosc 1999; 49:754–748.
24. Hildebrandt U, Klein T, Feifel G, et al. Endosonography of pararectal lymph nodes: in vitro and in vivo evaluation. Dis Colon Rectum 1990; 33:863–868.
25. Hildebrandt U, Feifel G. Importance of endoscopic ultrasonography staging for treatment of rectal cancer. Gastrointest Endosc Clin N Am 1995; 5:843–849.
26. Katsura Y, Yamada K, Ishizawa T, Yoshinaka H, Shimazu H. Endorectal ultrasonography for the assessment of wall invasion and lymph node metastasis in rectal cancer. Dis Colon Rectum 1992; 35:362–368.
27. Lee AS, Weissleder R, Brady TJ, Wittenberg J. Lymph nodes: microstructural anatomy at MR imaging. Radiology 1991; 178:519–522.
28. Improved survival with preoperative radiotherapy in resectable rectal cancer. Swedish Rectal Cancer Trial. N Engl J Med 1997; 336:980–987.
29. Kapiteijn E, Marijnen CA, Nagtegaal ID, et al. Preoperative radiotherapy combined with total mesorectal excision for resectable rectal cancer. N Engl J Med 2001; 345:638–646.